

# Hierarchical Graphene-Based Material for Over 4.0 Wt % Physisorption Hydrogen Storage Capacity

Chun Xian Guo,<sup>†,‡,⊥</sup> Yi Wang,<sup>§,‡</sup> and Chang Ming Li<sup>\*,†,||,⊥</sup>

<sup>†</sup>Institute for Clean Energy & Advanced Materials, Southwest University, Chongqing 400715, P.R. China

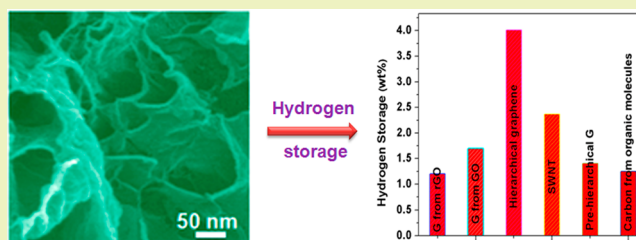
<sup>§</sup>National Engineering Laboratory for Hydrometallurgical Cleaner Production Technology, Institute of Process Engineering, Chinese Academy of Sciences, Beijing 100190, P.R. China

<sup>||</sup>School of Chemical and Biomedical Engineering & Centre for Advanced Bionanosystems, Nanyang Technological University, 70 Nanyang Drive, Singapore 637457, Singapore

<sup>⊥</sup>Chongqing Key Laboratory for Advanced Materials and Technologies of Clean Energies, Chongqing 400715, P.R. China

## S Supporting Information

**ABSTRACT:** A hierarchical graphene material composed of micropore ( $\sim 0.8$  nm), mesopore ( $\sim 4$  nm), and macropore ( $> 50$  nm) and with a specific surface area up to  $1305 \text{ m}^2 \text{ g}^{-1}$  is fabricated for physisorption hydrogen storage at atmospheric air pressure, showing a capacity over 4.0 wt %, which is significantly higher than reported graphene materials and all other kinds of carbon materials.



**KEYWORDS:** Graphene, Hierarchical structure, Nanopores, Hydrogen storage, Physisorption

Hydrogen is one of the most promising future sustainable energy fuels due to its abundance, high energy density, and environmental friendliness.<sup>1–6</sup> Nevertheless, its storage remains a great challenge for practical applications.<sup>7–10</sup> Carbon materials have recently attracted great attention in hydrogen storage in terms of their light weight, low cost, and unique chemical and physical properties related to the hydrogen storage.<sup>8,11</sup> Various carbons including activated carbons, mesoporous carbons, carbon black, and carbon nanotubes (CNTs) have been studied intensively.<sup>12–16</sup> Hydrogen storage by physisorption allows fast loading and unloading with low energy consumption and thus is a very promising approach in comparison to a chemisorption one.<sup>17,18</sup> However, the physisorption hydrogen storage of carbons at atmospheric air pressure is lower than 2.5 wt %, which is still far away from the target (6.5 wt %) set by the U.S. Department of Energy.<sup>19</sup>

Graphene-based materials are a relatively new member of the carbon family<sup>20–22</sup> and have very recently been explored for hydrogen storage.<sup>17</sup> As the physisorption interaction between graphene and hydrogen is dominated by weak van der Waals force, the amount of hydrogen stored in two-dimensional graphene nanosheets is relatively low ( $< 2.0$  wt %).<sup>15</sup> The theoretical studies of effects of nanostructures of graphene materials on hydrogen storage have predicted that nanopores less than 1 nm and a hierarchical structure are critical for the storage capacity improvement.<sup>19,23</sup> Inspired by the theoretical studies, herein we fabricated a hierarchical graphene-based material composed of micropore ( $\sim 0.8$  nm), mesopore ( $\sim 4$  nm), and macropore ( $> 50$  nm) with a Brunauer–Emmett–Teller (BET) surface area of up to  $1305 \text{ m}^2 \text{ g}^{-1}$ . The hydrogen

physisorption storage behavior on the hierarchical graphene-based material was investigated, showing a significantly enhanced capacity more than 4.0 wt % over the reported graphene materials and all other kinds of carbon materials as well.

The hierarchical graphene-based material was fabricated using a vacuum-based, low-temperature heating process followed by inert gas-protected thermal treatment. Graphite oxide was synthesized from graphite as reported.<sup>20</sup> Prehierarchical graphene-based material was prepared by placing the graphite oxide in a glass bottle to heat at  $150$  °C under vacuum for 45 min.<sup>24,25</sup> Hierarchical carbon-based material was then obtained by treating the prehierarchical graphene-based material in a quartz tube at  $600$  °C under Ar gas protection for at least 6 h, resulting in a highly loose and black powder.

The scanning electron microscopy (SEM) image in Figure 1a shows that the hierarchical graphene material is composed of micrometer-sized wavelike sheets. These wavelike sheets connect with each other to form a highly porous structure with pore sizes ranging from 50 to 200 nm. The detailed pore structure can be clearly seen from the high-magnification SEM image in Figure 1b, which has well-defined pores formed by wavy and contacted ultrathin graphene-based sheets. The transmission electron microscopy (TEM) image in Figure 1c illustrates that the material has a transparent nature, further confirming that it is made up of ultrathin sheets. The thickness

Received: July 5, 2012

Revised: August 22, 2012

Published: September 23, 2012

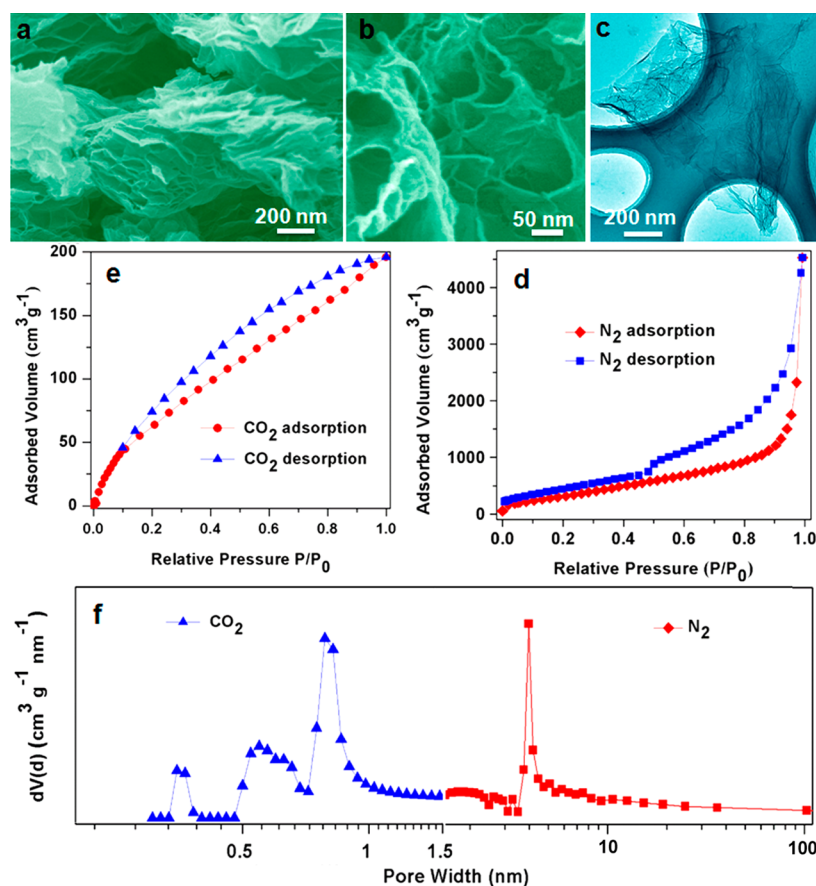


**Figure 1.** Characterizations of the hierarchical graphene-based material. (a, b) SEM and (c) TEM images. (d)  $N_2$  adsorption/desorption at 77 K. (e)  $CO_2$  adsorption/desorption at 273 K. (f) The corresponding pore size distributions.

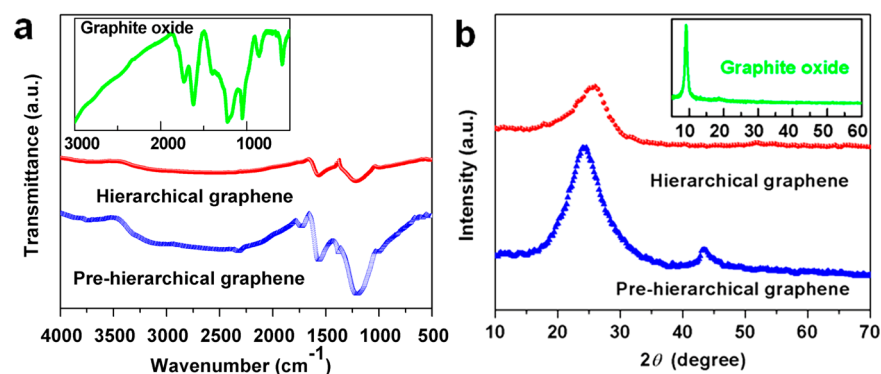


**Figure 2.** (a) Fourier transform infrared (FTIR) spectra and (b) X-ray diffraction (XRD) patterns of the hierarchical graphene-based material and pre-hierarchical graphene-based material.

of some individual graphene sheets obtained from sonication was examined by atomic force microscopy (AFM), exhibiting an average thickness of 0.9 nm (Figure S1, Supporting Information), which is the typical thickness of a graphene nanosheet.<sup>20</sup>

The specific surface area and mesopore structure (2–50 nm) of the material are investigated by  $N_2$  adsorption/desorption (77 K) experiment with the isotherms shown in Figure 1d. On the basis of the multipoint Brunauer–Emmett–Teller (BET) method, the calculated specific surface area is  $1305 \text{ m}^2 \text{ g}^{-1}$ , which is much higher than that of graphite ( $38 \text{ m}^2 \text{ g}^{-1}$ ),<sup>24</sup> CNTs ( $<200 \text{ m}^2 \text{ g}^{-1}$ ),<sup>25</sup> and other kinds of graphene materials.<sup>26</sup> The pore size distribution of the material has a

pronounced mesoporosity centered at 4 nm (Figure 1f). The BET method based on  $N_2$  adsorption/desorption is not suitable to characterize a small microporous structure ( $<1 \text{ nm}$ ).<sup>27</sup> Thus,  $CO_2$  adsorption/desorption experiment at 273 K was performed to investigate the ultramicropore (pores of width  $<1 \text{ nm}$ ) structure as shown in Figure 1e. The ultramicropore size was analyzed from  $CO_2$  adsorption/desorption isotherms by applying a Monte Carlo method.<sup>27</sup> The obtained pore size distribution from both  $CO_2$  and  $N_2$  adsorption/desorption isotherms indicates that the carbon material has significant ultramicropore (0.6–0.8 nm) and mesopore (4 nm) distributions. Combining with macropore ( $>50 \text{ nm}$ ) sizes ranging from 50 to 200 nm observed from the SEM characterizations shown

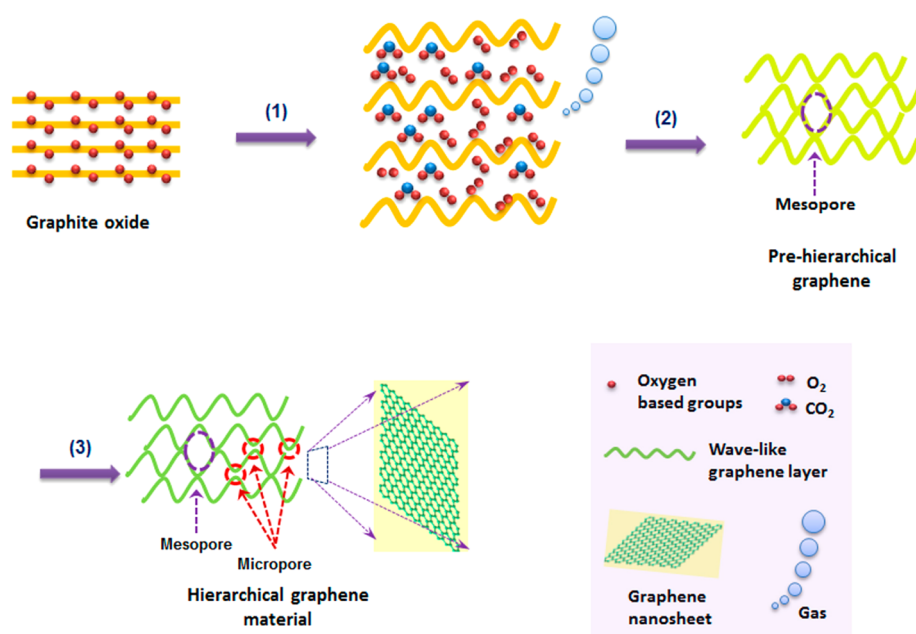


**Figure 3.** Scheme for the formation process of the hierarchical graphene-based material.

in Figure 1a and 1b, the material is indeed very distinctively hierarchically nanopore structured with a series of micro-, meso-, and macropores.

The formation mechanism for the hierarchical graphene-based material is analyzed based on the structure and surface property characterization results. The starting material of graphite oxide has abundant oxygen functional groups such as carboxyl and hydroxyl groups (inset of Figure 2a).<sup>28–30</sup> Heat treatment at a temperature of 150 °C under vacuum exfoliates graphite oxide, which is indirectly confirmed by the observation on an explosive-like phenomenon for dense graphite oxide to fluffy black powder. It is well-known that graphene sheets are flexible and have a very low density.<sup>27</sup> Under the exfoliated state, it is difficult for them to remain flat in a solid state, but rather maintain a bended form. We can reasonably argue that some oxygen functional groups under high temperature and vacuum could be converted to gas molecules such as O<sub>2</sub> and/or CO<sub>2</sub>. The gas escape can create pores between graphene sheets to form a wavelike structure. The release of gas molecules also can be directly proved from the increased pressure inside the glass tube that is connected to a pressure meter. The removal of most oxygen functional groups is also supported by the FTIR results shown in Figure 2a. During the exfoliation and cooling processes, wavelike graphene sheets collapse due to the strong  $\pi$ - $\pi$  interaction, resulting in the formation of pre-hierarchical graphene-based material with nanopores. The pre-hierarchical graphene-based material has a specific surface area around 480 m<sup>2</sup> g<sup>-1</sup> and a pore distribution of 4 nm (Figure S2, Supporting Information), while displaying almost negligible pores less than 1 nm (Figure S3, Supporting Information). Hierarchical carbon is obtained by further heat treatment of the pre-hierarchical carbon at a temperature of 600 °C under Ar gas protection. The further heat treatment reduces the surface functional groups (Figure 2a) and greatly increases the amount of micropores less than 1 nm in comparison to the pre-hierarchical graphene material for significantly increased specific surface area (1305 versus 480 m<sup>2</sup> g<sup>-1</sup>). The micropores are very likely to be formed from the space originally occupied by the surface functional groups (Figure 2a). In addition, powder X-ray

diffraction results shown in Figure 2b show that the (002) peak of the hierarchical graphene-based material has a markedly reduced intensity and is broadened, indicating that the hierarchical carbon is composed of many single- and several-layer nanosheets, which is consistent with the AFM characterization for graphene sheets observation (Figure S1, Supporting Information), which has a significantly different structure from that of expandable graphite materials. The formation process of the hierarchical carbon is schematically summarized in Figure 3.

Figure 4a presents hydrogen adsorption and desorption isotherms of the hierarchical carbon at 77 K with pressure up to 106.66 kPa. To better understand the hydrogen storage behavior on the hierarchical carbon, isotherms of the pre-hierarchical carbon are also shown in Figure 4a. The purity of the used hydrogen gas in the experiments is above 99.999%. Both materials exhibit an almost linear hydrogen uptake with respect to the pressure. The reversibility is assessed by measuring the desorption branch down to a very low pressure. From the isotherms in Figure 4a, it can be seen that the desorption branch nearly coincides with the adsorption branch, indicating that chemisorption is not the main mechanism for the hydrogen storage because a large desorption hysteresis loop is usually the prominent feature of chemisorptions.<sup>5</sup> The hierarchical carbon shows a higher hydrogen storage capacity of up to 4.01 wt %, which is almost three times higher than that of the pre-hierarchical carbon (1.40 wt %). In addition, the capacity is much higher than that for graphene prepared from exfoliated graphene oxide (1.70 wt %),<sup>14</sup> graphene-like nanosheets from reduced graphene oxide (1.20 wt %),<sup>15</sup> single-walled carbon nanotubes (2.37 wt %),<sup>13</sup> and carbon derived from chlorine-containing small organic molecules (1.25 wt %)<sup>16</sup> at similar testing conditions (Figure 4c).

To evaluate the interactions between the hierarchical carbon and hydrogen, the isosteric heats of adsorption are calculated from the adsorption isotherms at different temperatures of 77 and 87 K and are analyzed by Van't Hoff equation,<sup>31</sup> with the results shown in Figure 4b. The isosteric heat of adsorption on the pre-hierarchical carbon is also presented for comparison. It can be seen that, at low hydrogen coverage, the adsorption

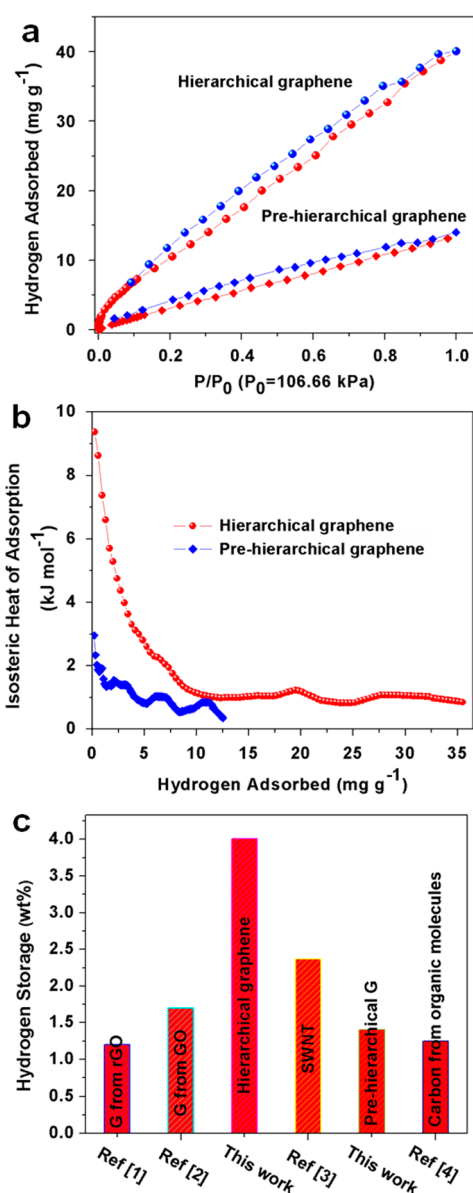


**Figure 4.** (a) Hydrogen adsorption and desorption isotherms of the hierarchical graphene and pre-hierarchical graphene. (b) Isosteric heat of hydrogen sorption. (c) Physisorption hydrogen storage capacity comparison between the hierarchical graphene and various carbon materials.

heats for both hierarchical and pre-hierarchical carbon are large. With the increased hydrogen coverage, the adsorption heat decreases quickly. This phenomenon corresponds to the adsorption in small pores with small volume fraction where the adsorption potential is high. The pre-hierarchical carbon has an adsorption heat of 2.9 kJ mol<sup>-1</sup> at a hydrogen capacity of 0 mg g<sup>-1</sup> and becomes relatively constant at ~1 kJ mol<sup>-1</sup> or less when hydrogen capacity is ~4 mg g<sup>-1</sup>. The hierarchical carbon has an adsorption heat of 9.5 kJ mol<sup>-1</sup> at a hydrogen capacity of 0 mg g<sup>-1</sup> and keeps relatively constant at ~1 kJ mol<sup>-1</sup> after hydrogen capacity exceeds 10 mg g<sup>-1</sup> until very high hydrogen coverage. The adsorption heats for both hierarchical and pre-hierarchical carbon are much lower than those reported for materials with chemisorptions.<sup>32</sup> It is also obvious that the hydrogen storage capacities for the two carbon materials do not result from the hydrogen spillover process because no active

catalyst is added. Thus, we can conclude that the hydrogen storage mechanism is mainly physisorption.

The hydrogen storage capacity of the hierarchical carbon (4.01 wt %) is nearly three times that of the pre-hierarchical carbon (1.40 wt %), which corresponds to their BET surface ratio, in which the BET surface area of the hierarchical carbon (1305 versus 480 m<sup>2</sup> g<sup>-1</sup>) is about 3 times that of the pre-hierarchical carbon. This correlation is in agreement with the reported conclusion that there is a linear relationship between the hydrogen storage capacity and the BET surface area for a physical adsorption mode.<sup>12</sup> This observation further confirms the physisorption in principle for the hierarchical carbon. Compared with pre-hierarchical carbon, the hierarchical material exhibits a much higher adsorption heat (9.5 versus 2.9 kJ mol<sup>-1</sup>) at the initial hydrogen coverage, possibly indicating that the small micropores (<1 nm) greatly enhance its hydrogen storage capacity. Therefore, the high hydrogen storage capacity of the hierarchical carbon should mainly result from the ultrahigh specific surface area and hierarchically nanoporous structure, in particular the small micropores less than 1 nm. The hierarchical nanopore structure including mesopore (~4 nm) and macropore (>50 nm) also should be helpful in hydrogen storage and release by providing efficient paths. Nevertheless, energetic sites including defect sites and edge sites (i.e., armchair and zigzag edge sites) and some functional groups on the hierarchical carbon should not be ruled out, which may partially contribute to the higher hydrogen storage capacity as compared with other carbon materials as shown in Figure 4c. Further experiments are designed and carried out in our lab for understanding their roles in the hydrogen storage capacity enhancement.

In summary, we report a graphene-based material with hierarchical nanopore structure comprising micropore (~0.8 nm), mesopore (~4 nm), and macropore (>50 nm) and with a specific surface area of up to 1305 m<sup>2</sup> g<sup>-1</sup>. The hierarchical graphene material demonstrates a physisorption hydrogen storage capacity of more than 4.0 wt %, which is significantly higher than that of reported graphene materials and all other kinds of carbon materials measured at the similar conditions. The hydrogen storage capacity for the hierarchical graphene material could further be improved by metal doping, surface functionalization, and edge-site tailoring for the practical applications, and these are currently underway in our lab.

## ■ ASSOCIATED CONTENT

### 📄 Supporting Information

Experimental details. This material is available free of charge via the Internet at <http://pubs.acs.org>.

## ■ AUTHOR INFORMATION

### ✉ Corresponding Author

\*Fax: (+65) 6791 1761. E-mail: [ecmli@ntu.edu.sg](mailto:ecmli@ntu.edu.sg).

### 👤 Author Contributions

‡These authors contributed equally. The manuscript was written through contributions of all of the authors, and all of the authors have given approval to the final version of the manuscript.

### 💰 Funding

This work is supported by Institute for Clean Energy & Advanced Materials, Southwest University, Chongqing Key Laboratory for Advanced Materials and Technologies of Clean Energies and Chongqing Science and Technology Commission



(cstc2012gjh90002), as well as by One Hundred Talent Program of Chinese Academy Of Sciences.

## Notes

The authors declare no competing financial interest.

## REFERENCES

- (1) Choudhury, N. A.; Sampath, S.; Shukla, A. K. Hydrogel-polymer electrolytes for electrochemical capacitors: An overview. *Energy Environ. Sci.* **2009**, *2*, 55–67.
- (2) Chen, Y. J.; Wang, Q. S.; Zhu, C. L.; Gao, P.; Ouyang, Q. Y.; Wang, T. S.; Ma, Y.; Sun, C. W. Graphene/porous cobalt nanocomposite and its noticeable electrochemical hydrogen storage ability at room temperature. *J. Mater. Chem.* **2012**, *22*, 5924–5927.
- (3) Almasoudi, A.; Mokaya, R. Preparation and hydrogen storage capacity of templated and activated carbons nanocast from commercially available zeolitic imidazolate framework. *J. Mater. Chem.* **2012**, *22*, 146–152.
- (4) Reich, T. E.; Jackson, K. T.; Li, S.; Jena, P.; Ei-Kaderi, H. M. Synthesis and characterization of highly porous borazine-linked polymers and their performance in hydrogen storage application. *J. Mater. Chem.* **2011**, *21*, 10629–10632.
- (5) Wang, Y.; Liu, J. H.; Wang, K.; Chen, T.; Tan, X.; Li, C. M. Hydrogen storage in Ni–B nanoalloy-doped 2D graphene. *Int. J. Hydrogen Energy* **2011**, *36*, 12950–12954.
- (6) Wang, Y.; Guo, C. X.; Wang, X.; Guan, C.; Yang, H. B.; Wang, K.; Li, C. M. Hydrogen storage in a Ni–B nanoalloy-doped three-dimensional graphene material. *Energy Environ. Sci.* **2011**, *4*, 195–200.
- (7) Wang, L. F.; Stuckert, N. R.; Chen, H.; Yang, Y. T. Effects of Pt particle size on hydrogen storage on Pt-doped metal–organic framework IRMOF-8. *J. Phys. Chem. C* **2011**, *115*, 4793–4799.
- (8) Schlapbach, L.; Zuttel, A. Hydrogen-storage materials for mobile applications. *Nature* **2001**, *414*, 353–358.
- (9) Jin, R. C.; Chen, G.; Wang, Q.; Sun, J. X.; Wang, Y. A facile solvothermal synthesis of hierarchical Sb<sub>2</sub>Se<sub>3</sub> nanostructures with high electrochemical hydrogen storage ability. *J. Mater. Chem.* **2011**, *21*, 6628–6635.
- (10) Mu, L.; Liu, B.; Liu, H.; Yang, Y. T.; Sun, C. Y.; Chen, G. J. A novel method to improve the gas storage capacity of ZIF-8. *J. Mater. Chem.* **2012**, *22*, 12246–12252.
- (11) Martin, N.; Guldi, D. M.; Hirsch, A. Carbon nanostructures for energy. *Energy Environ. Sci.* **2011**, *4*, 604–604.
- (12) Ströbel, R.; Garche, J.; Moseley, P. T.; Jörissen, L.; Wolf, G. Hydrogen storage by carbon materials. *J. Power Sources* **2006**, *159*, 781–801.
- (13) Nishimiya, N.; Ishigaki, K.; Takikawa, H.; Ikeda, M.; Hibi, Y.; Sakakibara, T.; Matsumoto, A.; Tsutsumi, K. Hydrogen sorption by single-walled carbon nanotubes prepared by a torch arc method. *J. Alloys Compd.* **2002**, *339*, 275–282.
- (14) Ghosh, A.; Subrahmanyam, K. S.; Krishna, K. S.; Datta, S.; Govindaraj, A.; Pati, S. K.; Rao, C. N. R. Uptake of H<sub>2</sub> and CO<sub>2</sub> by graphene. *J. Phys. Chem. C* **2008**, *112*, 15704–15707.
- (15) Srinivas, G.; Zhu, Y.; Piner, R.; Skipper, N.; Ellerby, M.; Ruoff, R. Synthesis of graphene-like nanosheets and their hydrogen adsorption capacity. *Carbon* **2010**, *48*, 630–635.
- (16) Jin, Z.; Sun, Z.; Simpson, L. J.; O'Neill, K. J.; Parilla, P. A.; Li, Y.; Stadie, N. P.; Ahn, C. C.; Kittrell, C.; Tour, J. M. Solution-phase synthesis of heteroatom-substituted carbon scaffolds for hydrogen storage. *J. Am. Chem. Soc.* **2010**, *132*, 15246–15251.
- (17) Wang, L.; Stuckert, N. R.; Yang, R. T. Unique hydrogen adsorption properties of graphene. *AIChE J.* **2011**, *57*, 2902–2908.
- (18) Rzepka, M.; Lamp, P.; de la Casa-Lillo, M. A. Physisorption of hydrogen on microporous carbon and carbon nanotubes. *J. Phys. Chem. B* **1998**, *102*, 10894–10898.
- (19) Dimitrakakis, G. K.; Tylianakis, E.; Froudakis, G. E. Pillared graphene: A new 3-D network nanostructure for enhanced hydrogen storage. *Nano Lett.* **2008**, *8*, 3166–3170.
- (20) Guo, C. X.; Yang, H. B.; Sheng, Z. M.; Lu, Z. S.; Song, Q. L.; Li, C. M. Layered graphene/quantum dots for photovoltaic devices. *Angew. Chem., Int. Ed.* **2010**, *49*, 3014–3017.
- (21) Guo, C. X.; Guai, G. H.; Li, C. M. Graphene based materials: Enhancing solar energy harvesting. *Adv. Energy Mater.* **2011**, *1*, 448–452.
- (22) Guo, C. X.; Li, C. M. A self-assembled hierarchical nanostructure comprising carbon spheres and graphene nanosheets for enhanced supercapacitor performance. *Energy Environ. Sci.* **2011**, *4*, 4504–4507.
- (23) Du, A.; Zhu, Z.; Smith, S. C. Multifunctional porous graphene for nanoelectronics and hydrogen storage: New properties revealed by first principle calculations. *J. Am. Chem. Soc.* **2010**, *132*, 2876–2877.
- (24) Guo, C. X.; Lu, Z. S.; Lei, Y.; Li, C. M. Ionic liquid–graphene composite for ultratrace explosive trinitrotoluene detection. *Electrochem. Commun.* **2010**, *12*, 1237–1240.
- (25) Hu, F. P.; Shen, P. K.; Li, Y. L.; Liang, J. Y.; Wu, J.; Bao, Q. L.; Li, C. M.; Wei, Z. D. Highly stable Pd-based catalytic nano-architectures for low temperature fuel cells. *Fuel Cells* **2008**, *8*, 429–435.
- (26) Lv, W.; Tang, D. M.; He, Y. B.; You, C. H.; Shi, Z. Q.; Chen, X. C.; Chen, C. M.; Hou, P. X.; Liu, C.; Yang, Q. H. Low-temperature exfoliated graphenes: Vacuum-promoted exfoliation and electrochemical energy storage. *ACS Nano* **2009**, *3*, 3730–3736.
- (27) Zhu, Y. W.; Murali, S.; Stoller, M. D.; Ganesh, K. J.; Cai, W. W.; Ferreira, P. J.; Pirkle, A.; Wallace, R. M.; Cychosz, K. A.; Thommes, M.; Su, D.; Stach, E. A.; Ruoff, R. S. Carbon-based supercapacitors produced by activation of graphene. *Science* **2011**, *332*, 1537–1541.
- (28) Guo, C. X.; Zheng, X. T.; Lu, Z. S.; Lou, X. W.; Li, C. M. Biointerface by cell growth on layered graphene–artificial peroxidase–protein nanostructure for in situ quantitative molecular detection. *Adv. Mater.* **2010**, *22*, 5164–5167.
- (29) Guo, C. X.; Lei, Y.; Li, C. M. Porphyrin functionalized graphene for sensitive electrochemical detection of ultratrace explosives. *Electroanal.* **2011**, *23*, 885–893.
- (30) Wobkenberg, P. H.; Eda, G.; Leem, D. S.; de Mello, J. C.; Bradley, D. D. C.; Chhowalla, M.; Anthopoulos, T. D. Reduced graphene oxide electrodes for large area organic electronics. *Adv. Mater.* **2011**, *23*, 1558–1562.
- (31) Lachawiec, A. J.; Yang, R. T. Isotope tracer study of hydrogen spillover on carbon-based adsorbents for hydrogen storage. *Langmuir* **2008**, *24*, 6159–6165.
- (32) Subrahmanyam, K. S.; Kumar, P.; Maitra, U.; Govindaraj, A.; Hembaram, K.; Waghmare, U. V.; Rao, C. N. R. Chemical storage of hydrogen in few-layer graphene. *Proc. Natl. Acad. Sci. U.S.A.* **2011**, *108*, 2674–2677.